Comparing methods for mapping canopy chlorophyll content in a mixed mountain forest using Sentinel-2 data

Ali, Abebe Mohammed ; Darvishzadeh, Roshanak ; Skidmore, Andrew ; Gara, Tawanda W ; O'Connor, Brian ; Röösli, Claudia ; Heurich, Marco ; Paganini, Marc

Abstract: The Sentinel-2 Multi-Spectral Imager (MSI) has three spectral bands centered at 705, 740, and 783 nm wavelengths that exploit the red-edge information useful for quantifying plant biochemical traits. This sensor configuration is expected to improve the prediction accuracy of vegetation chlorophyll content. In this work, we assessed the performance of several statistical and physical-based methods in retrieving canopy chlorophyll content (CCC) from Sentinel-2 in a heterogeneous mixed mountain forest. Amongst the algorithms presented in the literature, 13 different vegetation indices (VIs), a non-parametric statistical approach, and two radiative transfer models (RTM) were used to assess the CCC prediction accuracy. A field campaign was conducted in July 2017 to collect in situ measurements of CCC in Bavarian forest national park, and the cloud-free Sentinel-2 image was acquired on 13 July 2017. The leave-one-out cross-validation technique was used to compare the VIs and the non-parametric approach. Whereas physical-based methods were calibrated using simulated data and validated using the in situ reference dataset. The statistical-based approaches, such as the modified simple ratio (mSR) vegetation index and the partial least square regression (PLSR) outperformed all other techniques. As such the modified simple ratio (mSR3) (665, 865) gave the lowest cross-validated RMSE of 0.21 g/m2 (R2 = 0.75). The PLSR resulted in the highest R2 of 0.78, and slightly higher RMSE =0.22 g/m2 than mSR3. The physical-based approach-INFORM inversion using look-up table resulted in an RMSE =0.31 g/m2, and R2 = 0.67. Although mapping CCC using these methods revealed similar spatial distribution patterns, over and underestimation of low and high CCC values were observed mainly in the statistical approaches. Further validation using in situ data from different terrestrial ecosystems is imperative for both the statistical and physical-based approaches' effectiveness to quantify CCC before selecting the best operational algorithm to map CCC from Sentinel-2 for long-term terrestrial ecosystems monitoring across the globe.

DOI: https://doi.org/10.1016/j.jag.2019.102037

Originally published at:
Ali, Abebe Mohammed; Darvishzadeh, Roshanak; Skidmore, Andrew; Gara, Tawanda W; O'Connor, Brian; Röösli, Claudia; Heurich, Marco; Paganini, Marc (2020). Comparing methods for mapping canopy chlorophyll content in a mixed mountain forest using Sentinel-2 data. International Journal of Applied Earth Observation and Geoinformation, 87:102037.
DOI: https://doi.org/10.1016/j.jag.2019.102037

Int J Appl Earth Obs Geoinformation 87 (2020) 102037

Contents lists available at ScienceDirect

Int J Appl Earth Obs Geoinformation

journal homepage: www.elsevier.com/locate/jag

Comparing methods for mapping canopy chlorophyll content in a mixed mountain forest using Sentinel-2 data

Abebe Mohammed Ali[a,b,*], Roshanak Darvishzadeh[a], Andrew Skidmore[a,c], Tawanda W. Gara[a,d], Brian O'Connor[e], Claudia Roeoesli[f], Marco Heurich[g,h], Marc Paganini[i]

[a] Faculty of Geo-Information Science and Earth Observation (ITC), University of Twente, P.O. Box 217, 7500 AE Enschede, the Netherlands
[b] Wollo University, Department of Geography and Environmental Studies, P.O Box 1145, Dessie, Ethiopia
[c] Department of Environmental Science, Macquarie University, NSW, 2106, Australia
[d] Department of Geography and Environmental Science, University of Zimbabwe, P.O Box MP167, Mt Pleasant, Harare, Zimbabwe
[e] UN Environment Programme World Conservation Monitoring Centre (UNEP-WCMC), 219 Huntingdon Road, Cambridge, CB3 0DL, UK
[f] University of Zürich UZH, Department of Geography, Remote Sensing Laboratories, Winterthurerstrasse 190, 8057 Zurich, Switzerland
[g] Department of Visitor Management and National Park Monitoring, Bavarian Forest National Park, 94481 Grafenau, Germany
[h] Chair of Wildlife Ecology and Wildlife Management, University of Freiburg, Tennenbacher Straße 4, Germany
[i] European Space Agency - ESRIN, Via Galileo Galilei, Casella Postale 64, 00044 Frascati RM, Italy

ARTICLE INFO

Keywords:
Canopy chlorophyll content (CCC)
Comparing methods
Statistical methods
Radiative transfer model inversion
SNAP toolbox
Sentinel-2

ABSTRACT

The Sentinel-2 Multi-Spectral Imager (MSI) has three spectral bands centered at 705, 740, and 783 nm wavelengths that exploit the red-edge information useful for quantifying plant biochemical traits. This sensor configuration is expected to improve the prediction accuracy of vegetation chlorophyll content. In this work, we assessed the performance of several statistical and physical-based methods in retrieving canopy chlorophyll content (CCC) from Sentinel-2 in a heterogeneous mixed mountain forest. Amongst the algorithms presented in the literature, 13 different vegetation indices (VIs), a non-parametric statistical approach, and two radiative transfer models (RTM) were used to assess the CCC prediction accuracy. A field campaign was conducted in July 2017 to collect *in situ* measurements of CCC in Bavarian forest national park, and the cloud-free Sentinel-2 image was acquired on 13 July 2017. The leave-one-out cross-validation technique was used to compare the VIs and the non-parametric approach. Whereas physical-based methods were calibrated using simulated data and validated using the *in situ* reference dataset. The statistical-based approaches, such as the modified simple ratio (mSR) vegetation index and the partial least square regression (PLSR) outperformed all other techniques. As such the modified simple ratio (mSR3) (665, 865) gave the lowest cross-validated RMSE of 0.21 g/m^2 (R^2 = 0.75). The PLSR resulted in the highest R^2 of 0.78, and slightly higher RMSE = 0.22 g/m^2 than mSR3. The physical-based approach-INFORM inversion using look-up table resulted in an RMSE = 0.31 g/m^2, and R^2 = 0.67. Although mapping CCC using these methods revealed similar spatial distribution patterns, over and underestimation of low and high CCC values were observed mainly in the statistical approaches. Further validation using *in situ* data from different terrestrial ecosystems is imperative for both the statistical and physical-based approaches' effectiveness to quantify CCC before selecting the best operational algorithm to map CCC from Sentinel-2 for long-term terrestrial ecosystems monitoring across the globe.

1. Introduction

Canopy chlorophyll content (CCC) is defined as "the total amount of chlorophyll *a* and *b* pigments in a contiguous group of plants per unit ground area" (Gitelson et al., 2005) often expressed in g/m^2. It is a product of leaf chlorophyll content, *i.e.*, chlorophyll content of a fresh green leaf per unit area (μg/cm^2) and leaf area index (LAI) (m^2 m^{-2})) that describes chlorophyll pigments distribution within the three-dimensional canopy surface (Darvishzadeh et al., 2008b). Thus, CCC determines the total photosynthetically active radiation absorbed by the canopy (Gitelson et al., 2015). CCC is one of the plant pigments that provide valuable information about plant physiology and ecosystem processes (functions), enabling ecologists, farmers, and decision-makers to assess the influence of climate change, and other anthropogenic and

* Corresponding author.
E-mail address: a.m.ali@utwente.nl (A.M. Ali).

https://doi.org/10.1016/j.jag.2019.102037
Received 11 October 2019; Received in revised form 9 December 2019; Accepted 18 December 2019
Available online 24 December 2019

natural factors on plant functions and adaptation (Féret et al., 2017). CCC is an essential input variable to terrestrial biosphere models for quantifying carbon and water fluxes (Luo et al., 2018), primary productivity (Houborg et al., 2013; Peng and Gitelson, 2011), and light use efficiency (Wu et al., 2012). Changes in CCC can be an indicator of plant disease, nutritional, and environmental stresses (Korus, 2013; Zhao et al., 2011; Inoue et al., 2012). Therefore, because of its importance to ecosystem function and its value as an indicator of ecosystem health, CCC is an essential variable to be monitored consistently in space and time (Li et al., 2014; Homolova et al., 2013).

Remote sensing (RS) offers a means of monitoring and evaluating terrestrial vegetation at a wide range of spatial and temporal scales. Chlorophyll content at the leaf, canopy and landscape scales has been monitored using ground and airborne hyperspectral sensors and spaceborne satellites for the last four decades (*e.g.*, Darvishzadeh et al., 2008b; Asner et al., 2014; Houborg et al., 2015; Croft et al., 2013). Remote sensing is becoming the most popular means to retrieve chlorophyll content over large areas, by establishing empirical relationships between different vegetation indices (VIs) and chlorophyll content, or through physical-based approaches relying on the inversion of canopy reflectance models. Remote sensing of CCC is mainly based on optical remote sensing, covering the visible to near-infrared (NIR) spectral region, and the short wave infrared region (SWIR) as well when LAI and other vegetation biophysical properties effect is high (Inoue et al., 2016; Darvishzadeh et al., 2008c).

Concurrently with the evolution of satellite sensors, which bring increased resolution and sensitivity to biochemical variables, a number of robust algorithms have been developed that relate CCC and remote sensing data (*e.g.*, Vincini et al., 2016; Dian et al., 2016; Li et al., 2015; Ma et al., 2014; Verrelst et al., 2012). Notably, the red edge region (680–760 nm) of the reflectance spectrum also known as Red Edge Position (REP), has been widely used to estimate chlorophyll content from reflectance spectra (*e.g.*, Okuda et al., 2016; Li et al., 2016; Inoue et al., 2016) based on the fact that an increase in chlorophyll content will be reflected in the spectra by a shift in the absorption feature to longer wavelengths (Curran, 1989).

Plant canopy variables that can be predicted from remote sensing data include biophysical variables such as leaf area index (LAI), the fraction of vegetation cover (FVC), and biochemical variables such as water and dry matter content, carotenoid content, as well as CCC. Popular approaches that have been developed as ways of quantifying biophysical and biochemical variables from remote sensing data are typically grouped into two categories in the RS literature: (1) the statistical (variable-driven) category; and (2) physical-based (radiometric data-driven) category (Baret and Buis, 2008; Darvishzadeh et al., 2008c). They can also be characterized as inductive and deductive by their logic, or as deterministic and stochastic by their processing method (Skidmore, 2002). The increasing number of techniques in both approaches resulted in expanding the methodological categories into subcategories and combinations thereof (Verrelst et al., 2015). Hence, the later authors categorize the techniques into (i) parametric regression, (ii) non-parametric, (iii) physically-based, and (iv) combined methods.

Parametric regression methods are based on the relationship between spectral observations and a specific variable (e.g., CCC). These are inductive/empirical techniques used to find a statistical relation between the *in situ* measured plant trait and its spectral reflectance or some transformation of reflectance, *e.g.*, to a vegetation index, through fitting a function (Skidmore, 2002). The different forms of VIs and parametric approaches based on quasi-continuous spectral band configurations such as REP calculations and continuum removal are grouped under this category. Many reliable and robust VIs (*e.g.*, SAVI (Huete, 1988), TSAVI (Baret et al., 1989), TCARI (Haboudane et al., 2002), and MCARI (Daughtry et al., 2000) that are less affected by non-vegetated environmental factors have been developed for the inversion of plant properties from remote sensing data. The main advantage of parametric regression methods is their inherent simplicity, speed, and low computational expense. However, the downsides are data acquisition time, vegetation type and site-specific, and lacking generalization for upscaling approaches (*e.g.*, Cui and Zhou, 2017; Liang et al., 2016; Broge and Leblanc, 2001). These methods are based on a subset of spectral bands and make poor use of the large spectral information obtained from hyperspectral, and even multispectral sensors (Haboudane et al., 2004).

Unlike parametric regression methods, the non-parametric approaches do not rely on statistical distribution in the data. The optimization of non-parametric models makes use of a learning phase based on training data. A linear or non-linear fitting function is directly defined according to information from RS spectral data. The non-parametric models include stepwise multiple linear regression, principal components regression, partial least squares regression (PLSR), ridge (regulated) regression, decision tree learning (*e.g.*, random forest regression), artificial neural networks (ANN), kernel methods (*e.g.*, support/relevance vector machines), and kernel ridge regression, Gaussian process regression, and Bayesian networks. Detail description of each method can be found in Verrelst et al. (2015). Non-parametric models are computationally demanding, require field data, exhibit overfitting stemming from overly complex models (Rocha et al., 2017), and tend to be sensor-specific (Verrelst et al., 2015).

Physically-based approaches apply physical laws through the establishment of cause-effect relationships. The transfer and interaction of radiation energy inside the canopy can be described by canopy radiative transfer models (RTM) coupled with leaf-level physical models such as PROSPECT (Jacquemoud and Baret, 1990) and LIBERTY (Dawson et al., 1998) to derive leaf biochemistry. Radiative transfer inversion based methods are especially important in the case of heterogeneous environments, where canopy structure plays a significant role in the scattering processes (Widlowski et al., 2015; Yanez-Rausell et al., 2015). A large variety of canopy RTMs are currently available, and a recent inter-comparison is presented by Widlowski et al. (2015). RTMs range from the turbid medium models (1D) to Monte Carlo ray tracing three-dimensional (3D) models and their combinations. Inversion of RTMs can be performed using techniques such as a look-up table (LUT), iterative numerical optimization methods, or parametric and non-parametric approaches. The inversion of a canopy RTM is often considered as a physically sound approach because the approach is generic and has more transferability (Féret et al., 2011; Atzberger et al., 2013; Verrelst et al., 2010; Malenovský et al., 2008). However, the retrieval of variables through RTM inversion may be ill-posed (Combal et al., 2003) since different combinations of the input parameters may produce the same spectral signature. RTMs are also computationally demanding and require a large number of leaf and canopy variables, which need extra effort to acquire. Uncertainties emanating from measurements and model assumptions are prevailing in RTM inversion (Scales and Tenorio, 2001).

The fourth category of approaches combine elements of statistical approaches and physically-based models. They make use of the generic properties of physically-based methods combined with the flexibility and computational efficiency of parametric and non-parametric methods. RTMs are used to simulating canopy reflectance, and then the simulated data are used to train parametric or non-parametric methods to link spectral information and canopy parameters (Jacquemoud et al., 2009). Therefore, this approach has the advantage of empirical method simplicity as well as physical models universality. In contrast, they are often strongly affected by sensors and atmospheric noise and measurement uncertainty (Liang, 2007). The results of such methods also depend on the quality of the RTMs, and prior knowledge about input parameters (Verrelst et al., 2015).

Although numerous methods in all four categories have been proposed for estimating CCC (*e.g.*, Cui and Zhou, 2017; Liang et al., 2016; Atzberger et al., 2015; Darvishzadeh et al., 2008b), to date, there has been little agreement on a method that suitably applies to different

remote sensing data across different vegetation types. Accuracy of CCC prediction with different methods highly constrained by vegetation type (Zou et al., 2015; Niemann et al., 2012), spectral bands (Dian et al., 2016) and external factors (such as atmospheric condition and soil background) (Asner, 1998) as well as uncertainties associated with field/ground measurements of CCC. Discrepancies between remote sensing data acquired with different sensors, due to their spectral and spatial specifications, lead to various performances (*e.g.*, Darvishzadeh et al., 2019b) of the same method in predicting CCC. Therefore, the choice of the appropriate algorithm when predicting CCC and other vegetation traits is always a tradeoff decision between accuracy and efficiency.

While numerous studies have evaluated the performance of different approaches in estimating vegetation variables from hyperspectral remote sensing data (*e.g.*, Darvishzadeh et al., 2008b; Atzberger et al., 2010; Cui and Zhou, 2017), there has been limited effort towards examining the performance of these various methods to estimate CCC across different vegetation types using multispectral satellite remote sensing data such as Sentinel-2. The Sentinel-2 multi-spectral instrument (MSI) provides high spatiotemporal resolution and will generate long-term, continuous datasets with free access for current and future accurate global mapping of essential variables of terrestrial ecosystems, including canopy chlorophyll content. To our knowledge, only a few studies have evaluated the performance of Sentinel-2 data for predicting CCC in crops using statistical approaches (Clevers et al., 2017; Vincini et al., 2014; Chemura et al., 2017; Sun et al., 2018). Recently, Darvishzadeh et al. (2019a) evaluated the performance of a radiative transfer model (RTM) inversion in retrieving a temperate forest leaf chlorophyll content from Sentinel-2 and RapidEye.

This study aimed at evaluating the performance of the state-of-art methods for mapping CCC from Sentinel-2. Thus, our specific objectives were 1) through literature review, identify the highly recommended state-of-art methods and compare their accuracy, and precision in predicting CCC of a temperate heterogenous mountain forest from Sentinel-2 data, and 2) evaluate the consistency of the spatial distribution in the CCC products generated with the selected methods.

To achieve those objectives, methods that may be operationally feasible for large scale mapping of CCC were identified and shortlisted through a systematic literature review. Then the prediction performance of the candidate methods on Sentinel-2 MSI was validated by using *in situ* data. Finally, CCC spatial distribution maps were generated using the candidate methods that exhibit good performance and further evaluated for their spatial consistency.

2. Field data and methods

The overall procedures followed in comparing the different CCC retrieval algorithms are illustrated in Fig. 1. *In situ* CCC measurements and model input parameters' data were collected in 32 sample plots in the study area. Sentinel-2 image acquired during the field data collection was downloaded. Statistical-based methods were calibrated and validated by applying the leave-one-out cross-validation technique on the *in situ* measured CCC and their corresponding spectra from the Sentinel-2 data. In the case of physical-based models, RTMs were parameterized to simulate canopy reflectance, and inverted on Sentinel 2 data to predict CCC. RTM inversions' accuracy was then validated using the *in situ* measured CCC. Finally, the CCC products with relatively higher accuracy (higher correlation and lower error against *in situ* data) from each approach were checked for their spatial consistency, stability, and uniformity. The details of the field data collection and methods used are presented in the following subsections.

2.1. Test site

The test site for this study was the Bavarian Forest National Park in Germany (BFNP), which is located in south-eastern Germany, at center coordinates of 13°12′9″ E (longitude) and 49°3′19″ N (latitude) along the border between Germany to the Czech Republic. The Park is a mixed mountain forest with an approximate area of 240 km^2. Elevation varies between 600 m–1453 m. The park has a temperate climate. Annual precipitation range from 1200 mm to 1800 mm, with annual temperature averages from 3^0 to 6^0 Celsius. The lower altitude (below 900 m a.s.l) part of the park is predominated by brown soils, and in the high altitude area (above 900 m a.s.l), brown soils and brown podzolic soil are the predominant soil types (Heurich et al., 2010).

There are three ecological zones: Valleys, hillsides, and highlands. The natural forest ecosystems vary in each zone (Heurich et al., 2010). Alluvial spruce forests are dominant in the valleys, mixed mountain forests on the hillsides and mountain spruce forests in the high areas (Fig. 2). The European beech (*Fagus sylvatica*), Norway Spruce (*Picea abies*) and Fir (*Abies alba*) are the three dominant tree species. Sycamore Maple (*Acer pseudoplatanus L*), Mountain Ash (*Sorbus aucuparia L*), and Goat Willow (*Salix caprea*) are less often found in deciduous stands of the park (Heurich and Neufanger 2005). Due to massive disturbance by bark beetles and wind storms in recent decades, the forest structure in the park is very heterogeneous (Lehnert et al., 2013).

2.2. Data

2.2.1. In situ data

The CCC, field dataset was collected between 01 and 31 July 2017. The study area was stratified into Conifers, Broadleaf, and Mixed stands, and a random sampling technique was implemented to collect samples in each stratum. Biophysical and biochemical variables were obtained in total from 40 square plots with 30 m sides. Geographic coordinates of the plots were recorded at the center using a handheld Garmin Global Positioning System (GPS) that has a geometric accuracy within ± 5 m. In each plot, estimation of LAI and ALA were conducted using Li-COr LAI-2200 canopy analyzer equipment (LI-COR, 1992). We followed the standard procedure of taking one reference (above the canopy) reading in the nearest open field, and five below canopy measurements inside each plot in estimating LAI (Darvishzadeh et al., 2019a). A maximum effort was made to take the LAI-2200 measurements with constant illumination conditions for the above and below canopy readings.

In each plot, a crossbow was used to collect sample leaves/shoots from the mature sunlit part of the top of the canopy. Sample leaves/needles were collected from two to three branches of the representative trees in each plot. Leaves/shoots chlorophyll content were immediately measured using Chlorophyll Content Meter (CCM-300) and averaged to determine leaf chlorophyll content (C_{ab}) per plot. Then leaves/shoots were removed from the branches and placed in a zip-locked plastic bag together with wet pulp paper and transported to the laboratory. CCC of each plot was calculated by multiplying the plot's average C_{ab} and LAI. The summary of all the field data records is presented in Table 1.

2.2.2. Sentinel-2 data and pre-processing

To assess the CCC predictive accuracy of the different algorithms, the Sentinel-2A image of the study area acquired on 13 July 2017 was utilized. The image acquired on 13 July is chosen because the pilot site and its surroundings were cloud-free on this date. The Sentinel-2A level 1c product was downloaded from the ESA Copernicus. It has four bands at 10 m, six bands at 20 m, and three bands at 60 m spatial resolution in the visible and NIR and SWIR spectral regions. The three red-edge bands center at 705, 740, and 783 nm. Top-of-atmosphere (TOA) reflectance (level 1c product) was processed into top-of-canopy (TOC) reflectance (level 2A product) and resampled to 20 m spatial resolution using Sen2cor 2.5.5 stand-alone software, which is freely distributed under the GNU general public license (http://step.esa.int/main/third-party-plugins-2/sen2cor/). Spectral information from ten bands (band 2, 3, 4, 5, 6, 7, 8, 8a, 11, and 12) were utilized in this study. The remaining three bands (band 1, 9, and 10) serve mainly for atmospheric

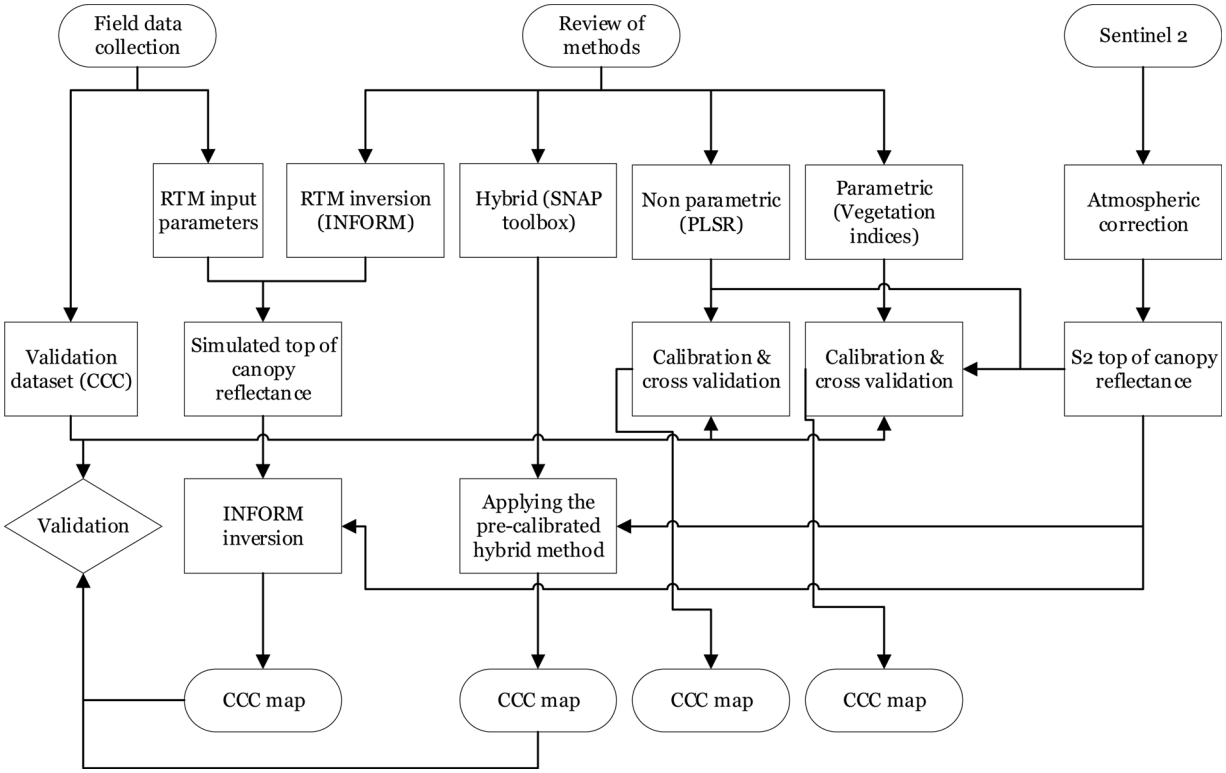

Fig. 1. Analytical framework for comparison of selected methods that can be used for the retrieval of CCC from Sentinel 2 surface reflectance data.

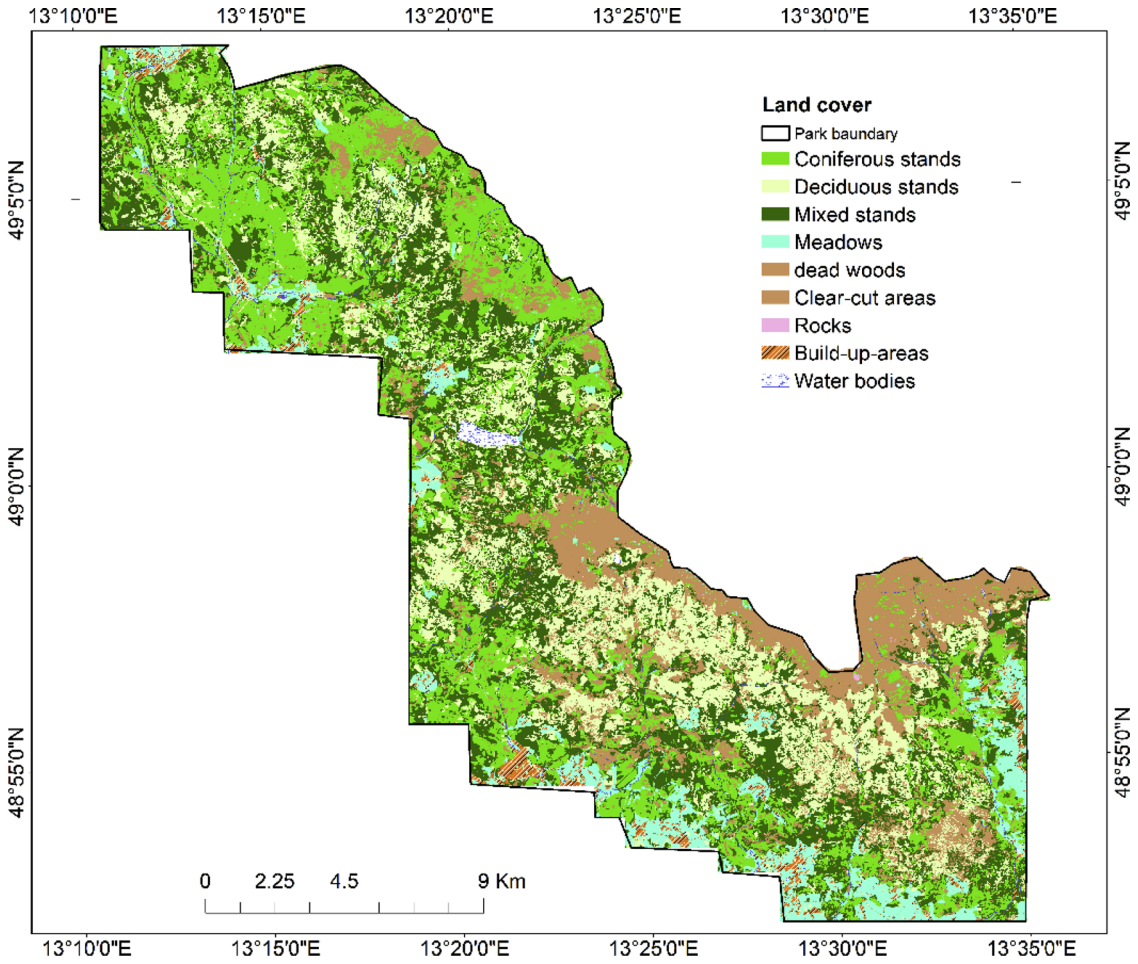

Fig. 2. Location and major vegetation types of Bavarian Forest National Park (source: Park administration office).

Table 1
Basic statistics of the *in situ* measured variables. Leaf chlorophyll content (C_{ab}), leaf area index (LAI), and Canopy chlorophyll content (CCC).

Summary	C_{ab} (μg cm^{-2})	LAI (m^2 m^{-2})	CCC (g m^{-2})
Minimum	33.62	1.33	0.58
Maximum	51.75	5.4	2.42
Mean	42.80	3.82	1.62
Std.dev	4.83	1.01	0.46

corrections and were not relevant for our purpose. The TOC reflectance data of the pixels containing the sample plots were extracted and used for testing the performance of the candidate algorithms together with *in situ* CCC.

2.3. CCC retrieval methods

Among the multitude of methods that have been proven to be superior when estimating CCC in a wide range of vegetation types in the literature, we selected some of the best-performing methods from each category to be evaluated for mapping CCC from Sentinel-2 data. Table 2 presents the proposed algorithm type and their formulation that are evaluated in the mixed mountain temperate forest of BFNP. Vegetation indices in the literature that use wavelengths closer to sentinel-2 band positions were considered.

2.3.1. Parametric and non-parametric approaches

The parametric and non-parametric methods were implemented with atmospherically corrected reflectance (TOC reflectance) obtained from the plot pixels. Linear or quadratic equations were fitted between the VIs and the *in situ* CCC depending on the nature of the relationship. In the case of Non-parametric approaches, different subsets of the spectral information in Sentinel-2 bands were tested. The number of components of the PLSR was optimized by testing different combinations of explanatory variables by adding an extra component to the models and observing Root Mean Square Error (RMSE) and Coefficient of determination (R^2) between the *in situ* and predicted values. Components that result in less than 2 % decrease in RMSE were ignored to avoid overfitting problems (Darvishzadeh et al., 2008c).

2.3.2. Physical-based model parameterization and inversion

2.3.2.1. Parameterization and generation of LUT using INFORM. The Invertible Forest Reflectance Model "INFORM" (Schlerf and Atzberger, 2006; Atzberger, 2001) is a combination of the forest light interaction model (Rosema et al., 1992) and SAIL (Verhoef, 1984) canopy RTMs with the PROSPECT leaf RTM (Jacquemoud and Baret, 1990). INFORM input parameters at the leaf level consist of C_m, C_w, C_{ab} and leaf Structure parameter (N), and at the canopy level include SD, single tree leaf area index (LAI_s), SH, CD, and ALA, as well as observation related parameters such as, view zenith (θ_o), sun zenith (θ_s) and relative azimuth angle (Φ). The model simulates top of canopy spectral reflectance of forest stands between the 400 and 2500 nm wavelengths.

To simulate the spectral property of forest ecosystems, the range of input parameters were determined using the field measurement, literature review, and sensor configurations (Table 3). In INFORM, LAI is represented by LAI_s. Hence, LAI_s was computed using eq.1 from LAI and CC (Schlerf and Atzberger, 2006).

$$LAI_s = \frac{LAI}{CC} \quad (1)$$

A LUT of canopy reflectance spectra is generated by varying the input parameters randomly within their range. For each spectra in the LUT, its corresponding CCC was computed and stored as a product of C_{ab} and LAI of the input parameters. The size of the LUT should be large enough so that the simulated spectra contain all possible combinations of the input parameters. However, if the LUT is extremely large, the inversion becomes computationally expensive. Therefore, a LUT of

Table 2
Methods tested for their performance to predict CCC from Sentinel-2 top of canopy reflectance data. *R* is the Sentinel-2 reflectance in different spectral bands.

Category	Algorithm	Original Formula	Formula on S2 bands	Reference
Parametric Statistical approach (vegetation indices)	The green Chlorophyll index (CI_{green})	$\frac{R_{780\,nm}}{R_{550\,nm}} - 1$	$\frac{R_{783\,nm}}{R_{560\,nm}} - 1$	Hunt et al. (2012)
	The red-edge chlorophyll index ($CI_{red\text{-}edge}$)	$\frac{R_{780\,nm}}{R_{705\,nm}} - 1$	$\frac{R_{783\,nm}}{R_{704\,nm}} - 1$	Gitelson et al. (2005)
	Simple Ratio Vegetation Index (SRVI)	$\frac{R_{815\,nm}}{R_{704\,nm}}$	$\frac{R_{835\,nm}}{R_{704\,nm}}$	Gitelson and Merzlyak (1997)
	modified Simple Ratio 2 (mSR2)	$\frac{R_{815\,nm}}{R_{704\,nm}}$	$\frac{R_{865\,nm}}{R_{704\,nm}}$	Gitelson and Merzlyak (1997)
	Modified Simple Ratio 3 (mSR3)	$\frac{R_{815\,nm}}{R_{704\,nm}}$	$\frac{R_{865\,nm}}{R_{665\,nm}}$	—
	Modified Simple Ratio 4 (mSR4)	$\frac{R_{815\,nm}}{R_{704\,nm}}$	$\frac{R_{835\,nm}}{R_{665\,nm}}$	—
	Datt Derivative (DD)	$\frac{DR_{754\,nm}}{DR_{704\,nm}}$	$\frac{DR_{740\,nm}}{DR_{704\,nm}}$	Datt (1999)
	MERIS Terrestrial Chlorophyll index (MTCI)	$\frac{R_{753.75} - R_{708.75}}{R_{708..75} - R_{681.25}}$	$\frac{R_{740} - R_{704}}{R_{704} - R_{665}}$	Dash and Curran (2004)
	modified MTCI (mMTCI)	$\frac{R_{753.75} - R_{708.75}}{R_{708..75} - R_{681.25}}$	$\frac{R_{665} - R_{497}}{R_{497} - R_{865}}$	—
	the novel Inverted Red-Edge Chlorophyll Index (IRECI)	$\frac{R_{NIR} - R_{red}}{R_{red1} / R_{red2}}$	$\frac{R_{783} - R_{665}}{R_{704} / R_{740}}$	Frampton et al. (2013)
	Sentinel 2 red edge position index (S2REP)	$705 + \frac{35 * [(0.5 * (R_{783} + R_{665}) - R_{705})]}{(R_{740} - R_{705})]}$	$705 + \frac{35 * [(0.5 * (R_{783} + R_{665}) - R_{704})]}{(R_{742} - R_{704})]}$	Vincini et al. (2014)
	MCARI/OSAVI	$\frac{(R_{750} - R_{705}) - 0.2(R_{750} - R_{550})\left(\frac{R_{750}}{R_{705}}\right)}{(1 + 0.16)\, x\, \frac{R_{750} - R_{705}}{R_{750} + R_{705} + 0.16}}$	$\frac{(R_{783} - \rho\lambda_{704}) - 0.2(\rho_{783} - \rho\lambda_{665})\left(\frac{R_{783}}{R_{704}}\right)}{(1 + 0.16)\, x\, \frac{R_{783} - R_{704}}{R_{783} + R_{704} + 0.16}}$	Wu et al. (2008)
	Normalized Difference Red Edge index (NDRE)	$\frac{R_{790} - R_{720}}{R_{790} + R_{720}}$	$\frac{R_{783} - R_{704}}{R_{783} + R_{704}}$	Barnes et al. (2000)
Non-parametric Statistical approach	Partial Least Square Regression (PLSR)			Sæbø et al. (2008)
Physical-based approach	INFORM inversion using LUT			Schlerf and Atzberger (2006)
Combined approach	PROSAIL inversion using ANN (SNAP toolbox)			Baret (2016)

Table 3
INFORM input parameters used to generate the LUT as defined based on literature review and sensor configuration (sentinel-2 MSI).

Parameter	Symbol	Unit	Range		Source
			Min	Max	
Leaf dry mass per area	C_m	g/cm^2	0.005	0.03	(Ali et al., 2016a)
Equivalent water thickness	C_w	g/cm^2	0.006	0.035	(Ali et al., 2016a)
Leaf structural parameter	N	NA	1	2.5	(Ali et al., 2016a)
Leaf chlorophyll content	C_{ab}	µg/cm^2	5	65	Field measurement
Single-tree LAI	LAI_s	NA	2	10	Ali et al. (2016b)
Understory LAI	LAI_u	NA	0.2	1	Field measurement
Stem density	SD	n/hr	200	2000	Ali et al. (2016b)
Stand height	SH	m	5	40	Ali et al. (2016b)
Crown diameter	CD	m	3	10	Ali et al. (2016b)
Average leaf angle	ALA	degree	40	60	Field measurement
Sun zenith angle	θ_s	degree	25	35	Sentinel 2 metadata
Observation zenith angle	θ_0	degree	0	15	Sentinel 2 metadata
Azimuth angle	Φ	degree	50	210	Sentinel 2 metadata
Scale		NA	0.5	1.5	(Schlerf and Atzberger, 2006)
***Fraction of diffused radiation	Sky1	fraction	0.1		(Schlerf and Atzberger, 2006)

200,000 builds was implemented (*e.g.*, Wang et al., 2017). A random Gaussian noise value of 0.3 % was added to each simulated spectrum to account for model uncertainties and reduce auto-correlation between the simulated reflectance spectrum and input variables.

2.3.2.2. INFORM inversion using Look-up table (LUT). Inversion of the LUT generated by INFORM involved matching the similarity between measured spectra (Sentinel-2) and simulated spectra (INFORM). Spectrum matching was performed using the least RMSE comparison of the measured and simulated spectra according to Eq. 2.

$$RMSE = \sqrt{\frac{\sum (R_{measured} - R_{modelled})^2}{n}} \quad (2)$$

where $R_{measured}$ is a Sentinel-2 reflectance at wavelength λ and $R_{modelled}$ is a simulated reflectance at wavelength λ in the LUT, and n is the number of wavelengths.

An average absolute error was computed between the INFORM simulation and the Sentinel-2 reflectance data, and different Sentinel-2 band subsets were evaluated for their performance. The inversion result obtained from the band subset with lower absolute error (0.02), was proposed as a threshold to identify well-simulated bands by Darvishzadeh et al. (2008b) and used in this study. The solution to the inverse problem is the set of input parameters corresponding to the reflectance in the database that provided the smallest RMSE. Because of the potential insufficiency in model formulation and parameterization, and noise related to calibration and pre-processing errors in the observed reflectance, the least RMSE solution might not necessarily provide the best estimates. For this reason, for each measured spectrum, the first 10, 100, 250, and 500 (q) closest matching spectra were selected from the LUT and validated. From the multiple available solutions (q), the final solution was chosen by comparing the performance of statistical measures of central tendency such as mean, median, and mode of the closest matching spectral subsets. Then, the corresponding CCC value of the matching spectra was obtained as the final solution of the inversion.

2.3.3. A combined approach using the SNAP toolbox. The PROSAIL and artificial neural network (ANN) inversion approach have been implemented in the SNAP toolbox to generate biophysical products, including CCC from Sentinel-2 TOC reflectance (Baret, 2016). It uses an ANN trained on the PROSAIL simulated database. It requires an input layer of normalized TOC Sentinel-2 data: B3, B4, B5, B6, B7, B8a, B11, B12, cos(viewing zenith), cos(sun zenith), and cos(relative azimuth angle) and derives a set of biophysical variables, namely: leaf area index, fraction of absorbed photosynthetically active radiation, fraction of vegetation cover, chlorophyll content in the leaf and canopy water content. Then the CCC is computed as a product of C_{ab} and LAI. Details of the algorithm can be found in Baret (2016).

2.4. Validation

For parametric and non-parametric statistical approaches, a leave-one-out cross-validation procedure (Zhang, 2001) was performed using the *in situ* measured CCC of the sample plots (n = 32) and their corresponding TOC reflectance extracted from Sentinel-2 data. In the leave-one-out cross-validation approach, the calibration set of n-1 samples is used to fit the predictive model and then evaluated using the sample that has been left out.

In the case of INFORM inversion and the biophysical retrieval approach from the SNAP toolbox, the retrieved CCC values were validated using the *in situ* measured CCC of the sample plots. R^2, RMSE, and bias between the measured and predicted CCC was used to assess the accuracy of the methods. Boxplot and paired *t*-test were used to show how the predictions were in agreement with each other, and with the *in situ* CCC.

2.5. Mapping CCC

Before mapping CCC, the non-forested part of the test site (BFNP) was masked out from the Sentinel-2 image using a vegetation map obtained from the national park administration (Silveyra Gonzalez et al., 2018), which was a product of LiDAR and high-resolution imagery integration for object-based mapping of forest habitat. In this study, the forest includes conifer and broadleaf stands or a mix of the two with tree height ≥ 3 m. Once the forest area of the test site extracted, the best-performing methods from each category were applied to map CCC of the mixed mountain forest. The maps generated using the selected methods were compared for their stability, uniformity, and constancy by computing image difference and consistency statistics such as frequency distribution, range, and standard deviation.

3. Results

3.1. Calibration of the selected methods

All the tested vegetation indices showed markedly strong linear positive correlation (r) to CCC (Fig. 3a) ($p \leq 0.01$). The maximum r = 0.88 was observed for three VIs, namely mSR3, mSR2, and $CI_{red\ edge}$. Relatively lower r = 0.72 was obtained for S2REP. Fig. 3b–d demonstrated the nature of the relationship, the equation fitted, and the R^2 between the top three VIs against the measured CCC data. Other VIs correlation to measured CCC can be seen in Appendix A.

The non-parametric method-PLSR was trained on three spectral subsets: 1) red-edge bands of sentinel-2 (band 5, 6 and 7), 2) using all the valid ten bands described in Section 2.2.2 and 3) using eight spectral band subsets (band 2, 3, 4, 5, 6, 8a, 11 & 12) that showed higher variable importance in the prediction (result not shown here). Applying the criterion of change of RMSE ≥ 2 % to avoid overfitting, and to determine the most appropriate number of components resulted in a PLSR model with five components (using a spectral subset of eight bands of Sentinel-2) for accurate CCC retrieval.

Similarly, the performance of different spectral subsets was evaluated for inversion of INFORM on Sentinel-2 spectral bands. The results revealed that INFORM inversion using spectral information in the red and red-edge region, where an increase in chlorophyll content increases absorption, is the optimal subset. Therefore, inversion of INFORM on Band 4, Band 5 and Band 6 of Sentinel-2 showed high sensitivity to *in*

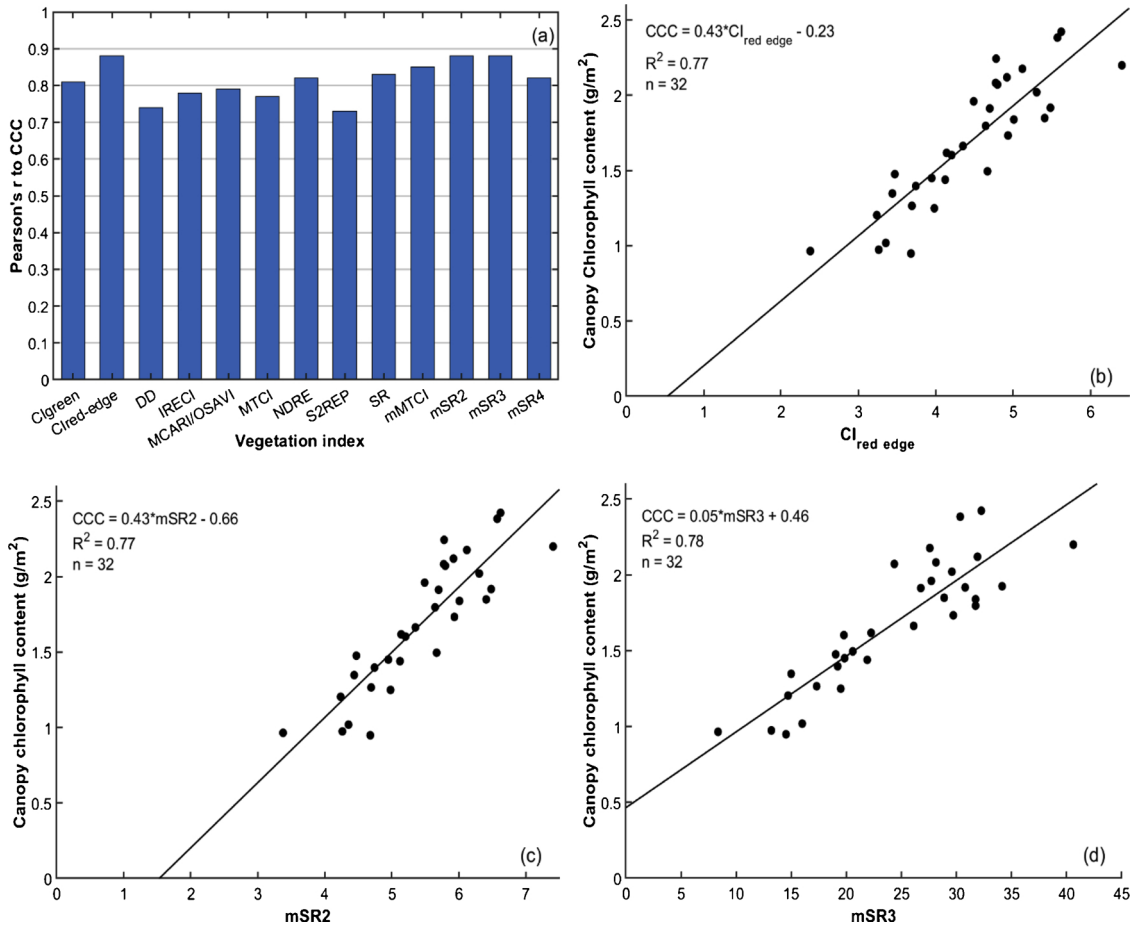

Fig. 3. Relationship between measured canopy chlorophyll content (CCC) (n = 32) and selected vegetation indices (VIs). (a) Bar graph of the VIs' Pearson correlation to CCC, (b–d) the scatterplot of CCC against the three best performings VIs.

Table 4
Accuracy of the estimates of CCC in the Bavarian forest national park obtained using the selected methods on Sentinel-2 data. Methods with better performance from each category (parametric and non-parametric statistical models, physical-based models, and their combination) are in bold. The R^2, RMSE, and bias are based on leave one out cross-validation approach for the statistical approach, and the whole *in situ* data for physical-based methods.

Category	Algorithm	R^2	RMSE (g/m2)	RMSE (%)	Bias
Parametric Statistical approaches (vegetation indices)	CI_{green}	0.61	0.25	15.58	−0.034
	$CI_{red\text{-}edge}$	0.74	0.23	13.57	0.026
	SR	0.69	0.24	14.69	0.038
	mSR2	0.74	0.23	13.57	0.026
	mSR3	**0.75**	**0.21**	**12.53**	**−0.016**
	SR4	0.65	0.25	15.22	0.006
	DD	0.50	0.29	17.36	0.003
	MTCI	0.55	0.30	17.53	0.032
	mMTCI	0.68	0.25	14.09	−0.003
	IRECI	0.58	0.26	15.18	0.030
	S2REP	0.48	0.29	17.11	0.046
	MCARI/OSAVI	0.57	0.26	15.44	0.032
	NDRE	0.63	0.25	14.56	0.028
Non-parametric Statistical approaches	PLSR) using red edge bands	0.67	0.24	14.32	−0.010
	PLSR using eight bands	**0.78**	**0.22**	**13.10**	**−0.038**
	PLSR using ten bands	0.74	0.21	12.49	−0.008
Physical approach	**Inversion of INFORM uing LUT**	**0.67**	**0.31**	**18.11**	**−0.101**
Combined approach	**SNAP toolbox**	**0.66**	**0.35**	**21.72**	**−0.1632**

situ measured CCC compared to any other spectral subset as well as the whole spectral dataset. From the multiple available solutions (q), we chose the median CCC value of the first 100 multiple solutions as a final solution after experimenting with the performance of the statistical measures of central tendency for the different closest matching spectral subsets.

3.2. Validation

Many of the statistical-based methods provide high R^2 and low RMSE/Bias combinations. The coefficient of determination between the measured and predicted CCC values range from 0.48 to 0.78 (Table 4). The highest R^2 was observed when PLSR applied to eight spectral bands

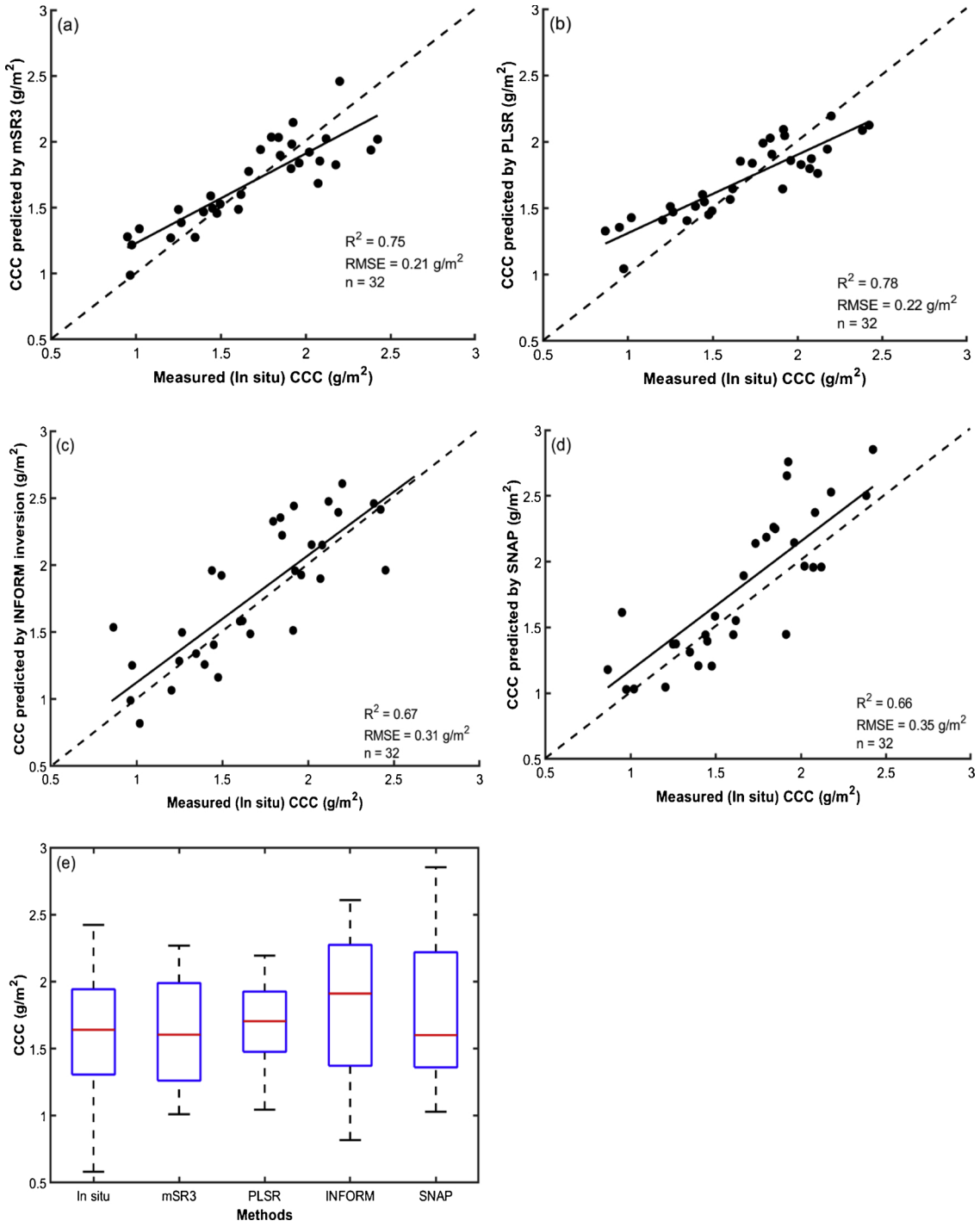

Fig. 4. (a–d) scatter plot of the *in situ* CCC and predictions made by the four methods and (e) their corresponding boxplot. In Figures a–d, the broken line shows the 1:1 relationship, while the solid line indicates the relationship between the field measured and predicted values of CCC.

Table 5
Paired *t*-test score of each selected method (*i.e.*, mSR3, PLSR, INFORM, and SNAP) predicted values against *in situ* CCC.

Method	Std. dev.	95 % conf. interval		tstat	p-value
		Lower	Upper		
mSR3	0.23	−0.08	0.08	−0.05	0.96
PLSR	0.40	−0.23	0.054	−1.27	0.21
INFORM	0.57	−0.38	0.03	−1.73	0.09
SNAP	0.32	−0.28	−0.05	−2.90	0.01

subset ($R^2 = 0.78$), and the minimum ($R^2 = 0.48$) for S2REP. The mSR3 and the PLSR provided relatively the highest R^2 and the lowest RMSE combinations. All statistical methods showed a bias close to zero (Bias $\leq$ 0.05). Whereas, the physical-based models: INFORM inversion by LUT and the SNAP toolbox reveal relatively higher bias.

One method with relatively higher accuracy and robustness from each category was selected for further investigation. Thus, predictions made using the mSR3 from VIs, PLSR on eight sentinel-2 bands from nonparametric, the inversion of INFORM using LUT and the SNAP toolbox (which are shown in bold in Table 4) were compared for their statistical significance difference from *in situ* data and spatial

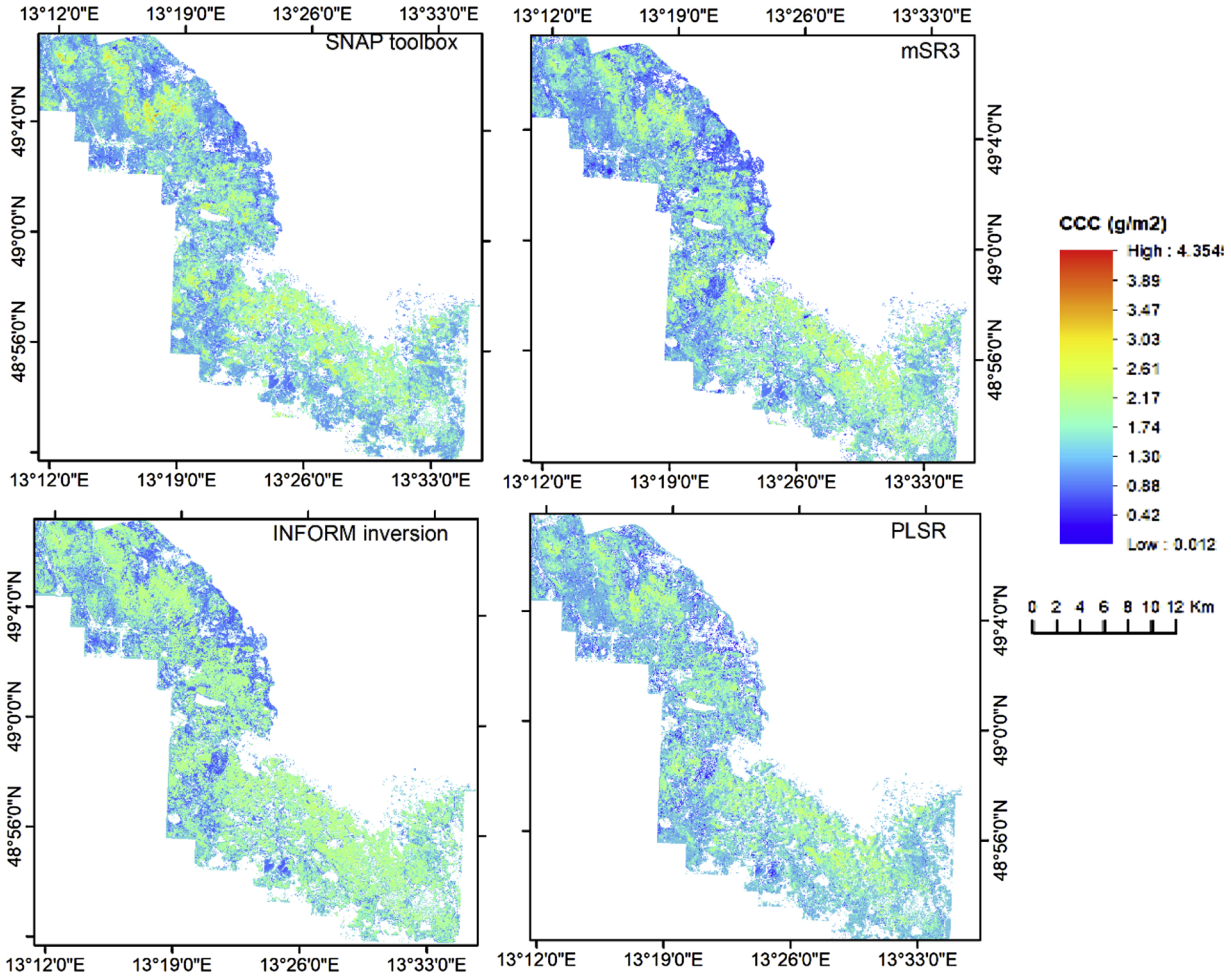

Fig. 5. CCC maps predicted from Sentinel-2 data by applying the SNAP toolbox approach, SRVI, INFORM inversion by LUT, PLSR, and PROSAIL inversion by LUT for Bavaria forest national park.

consistency. The scatterplots of predicted values obtained from the four approaches against the *in situ* CCC data are presented in Fig. 4 (see Appendix B for scatterplots of other methods). As can be observed from Fig. 4, the prediction is more accurate for the statistical-based approaches (Fig. 4a & b) than for physical-based model inversion (Fig. 4c & d). However, the statistical methods show a tendency to overestimate lower CCC values and underestimate higher CCC values, which is a sign of saturation problem due to the insensitivity of the methods for very low or high CCC values. The physical-based models avoided such saturation problems, and the predicted values were linearly scattered around the 1:1 relationship line (Fig. 4c & d). The Boxplot in Fig. 4e illustrates the summary of the central tendency of the four methods prediction compared to *in situ* CCC data. The analysis of paired *t*-test demonstrated (Table 5) that only prediction performed by the SNAP toolbox showed a significant difference from the *in situ* CCC ($p = 0.05$).

3.3. Mapping CCC and checking consistency

The similarities and differences of the spatial distribution of the predicted CCC by the selected methods were examined through visual inspection of the maps and computing basic statistics. Fig. 5 presents the spatial distribution map of the CCC across the study area (Bavarian Forest National Park) generated by using the four selected methods after masking non-forest land cover types using an existing land cover map of the study area. When compared to Fig. 6, the variability of CCC across different stands is visible in the four CCC products. Higher CCC are observed in deciduous stands (mean $= 1.77\ g/m^2$) than coniferous stands (mean $= 1.44\ g/m^2$) and mixed stands (mean $= 1.63\ g/m^2$) (Figs. 5 and 6). All methods, *i.e.*, the SNAP toolbox, SRVI (mSR3), INFORM inversion by LUT, and PLSR showed similar distribution with a higher frequency between 1 g/m^2 and 2 g/m^2 (Fig. 7).

The expected (obtained from the representative sample plots) and predicted CCC ranges in the four maps are presented in Table 6. It was observed that CCC predictions through INFORM inversion using LUT indicated a range, mean, and standard deviation much closer to the *in situ* data statistics than any other approaches. The highest CCC (4.35 g/m^2) was observed in the map produced using SNAP toolbox, and the lowest CCC (0.012 g/m^2) was recorded using the PLSR method. Consequently, the CCC product from the SNAP toolbox exhibited easily noticeable differences when compared to the other three CCC products (Fig. 8).

4. Discussion

This study compared the wide range of methods available in the literature for evaluating their operational feasibility in retrieving canopy chlorophyll content of a heterogeneous mixed mountain forest from the Sentinel-2 image. Although artefacts caused by canopy structure, radiometric distortions due to topography, atmosphere, solar illumination geometry, sensor viewing conditions, and soil optical

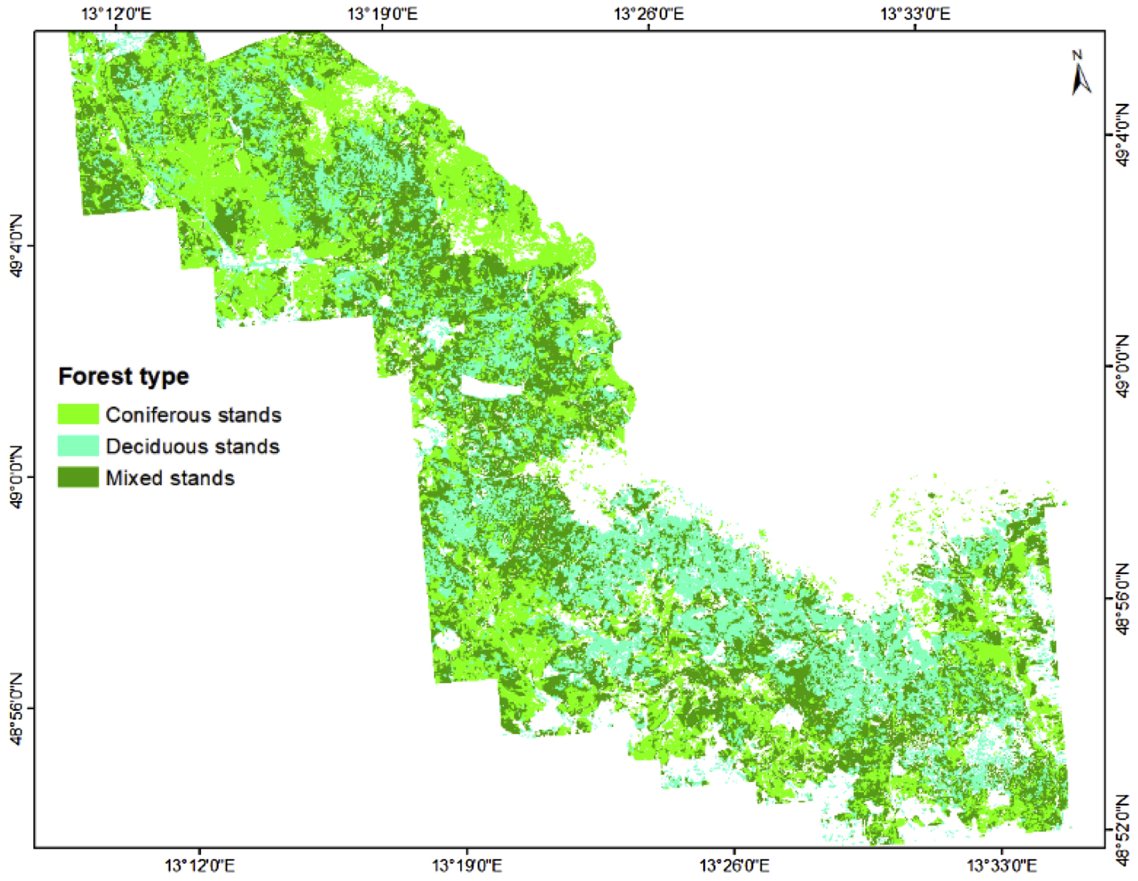

Fig. 6. The three forest stand types in the Bavarian national park.

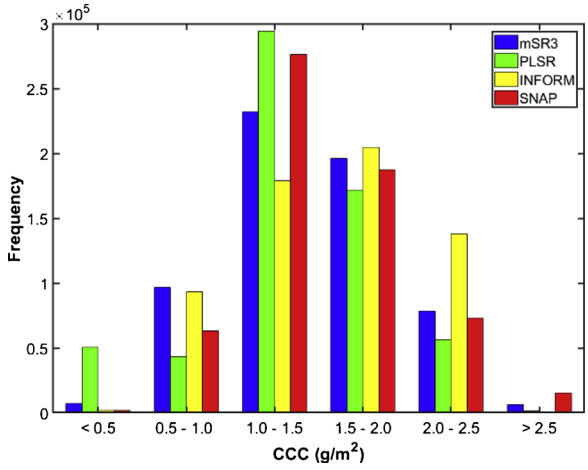

Fig. 7. The frequency distribution of CCC values of BFNP as predicted from Sentinel-2 data by applying the four methods (SRVI, PLSR, INFORM inversion by LUT, and SNAP toolbox approach.

Table 6
Summary statistics as a measure of consistency computed from the *in situ* data, and CCC maps produced by the four methods. Cells in bold show predicted CCC closer to expected values.

Method	minimum	Maximum	Mean	St. Dev
In situ	0.58	2.42	1.62	0.46
SRVI	0.26	2.80	1.46	0.47
PLSR	0.01	3.54	1.45	0.42
INFORM	**0.50**	**2.70**	**1.59**	**0.47**
SNAP toolbox	0.22	4.35	1.50	0.45

properties particularly in sparse vegetation, make retrieval of vegetation traits from canopy reflectance data challenging (Darvishzadeh et al., 2008a; Ollinger, 2011; Gitelson et al., 2005), many of the tested methods provided encouraging results to map CCC of the heterogeneous forest ecosystem.

Among the tested VIs, the simple ratio form of indices formulated based on wavelengths from the red-edge and NIR region showed good performance. CI_{red_edge} and mSR3 indices revealed the highest positive correlation (r = 0.88) to change in CCC (Fig. 3a and Appendix A) in this study. This was expected as spectra in the red-edge region have proven strong sensitivity to chlorophyll (*e.g.*, Ju et al., 2010; Dawson and Curran, 1998; Curran et al., 1990). Our finding agrees with several studies that reported the superior sensitivity of simple ratio vegetation indices to subtle changes in chlorophyll content (Inoue et al., 2016; Cui and Zhou, 2017; Tong and He, 2017).

Similarly, spectral subsets obtained from the red and red-edge region were the good fit spectral datasets for the inversion of RTMs. Also, PLSR calibration that includes this spectral region elucidated strong sensitivity to CCC. This finding broadly supports the work of other studies in this spectral region linking canopy reflectance with chlorophyll content acquired at leaf and canopy levels in forest ecosystems, grassland and crops (*e.g.*, Delegido et al., 2011; Clevers and Gitelson, 2012; Vincini et al., 2016; Darvishzadeh et al., 2019a).

The result showed that the mSR2, mSR3, and $CI_{red\text{-}edge}$ from the parametric statistical, PLSR from non-parametric statistical, INFORM inversion by using a LUT from physical-based, and the PROSAIL inversion by ANN (SNAP toolbox) from combined approaches were good predictors (Table 4). The highest R^2 was obtained by applying PLSR on eight selected spectral bands (R^2 = 0.78). However, the lowest RMSE was recorded for mSR3 (R^2 = 0.75, RMSE = 0.21 g/m^2). In terms of bias, among the good-performing methods in each category, relatively, the lowest bias was for mSR3 (bias = 0.016).

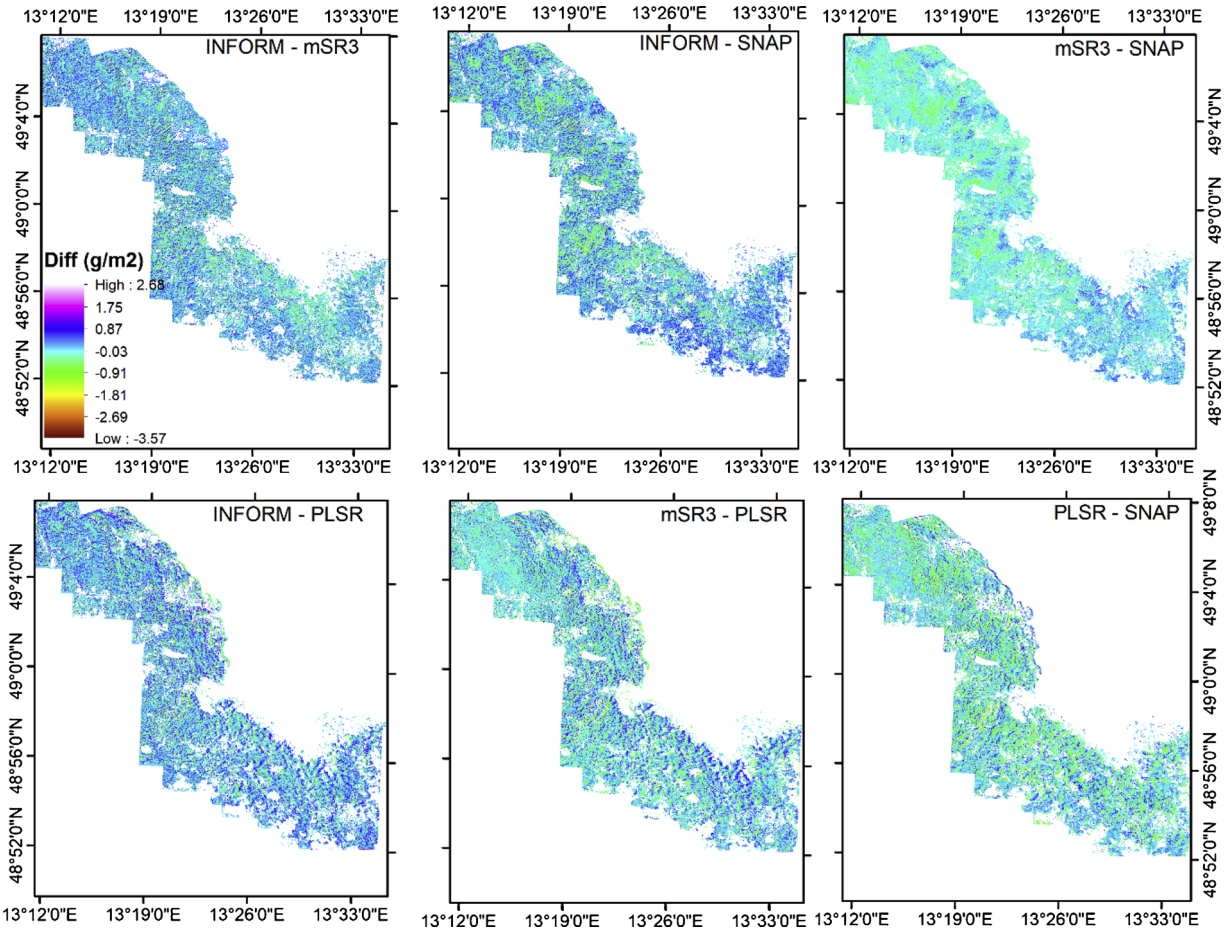

Fig. 8. Ddifference in canopy chlorophyll content (Diff) among products generated using the four methods. The differences are obtained by subtracting one product from another (*e.g.* the subtraction of mSR3 from INFORM based CCC product provided the map shown on the top left of the Figure).

Our results identified several VIs, applicable at Sentinel-2 spectral resolution, that can be used for computationally efficient prediction of CCC. Several studies have demonstrated VIs based on broadbands as useful predictors of chlorophyll content. For instance, Broge and Leblanc (2001) compared the prediction power and stability of broadband and hyperspectral VIs for estimation of LAI and canopy chlorophyll density, and concluded that hyperspectral indices are not necessarily better predictors of the two variables. The results from a study by Tong and He (2017) confirmed that broadband indices are as effective as narrowband indices for chlorophyll content estimation at both the leaf and canopy scale. Broge and Leblanc (2001) found broadband indices less affected by external factors such as canopy architecture, illumination geometry, soil background reflectance, and atmospheric conditions, and recommended for LAI and canopy chlorophyll content prediction. Nevertheless, VIs are based on empirical relationship, and may lack generality (*i.e.*, relationships being site, time, and species-specific) and caution should be taken when applying VIs developed for one vegetation type or time to another vegetation type or time (Haboudane et al., 2004; Verrelst et al., 2015; Atzberger et al., 2015).

Another important finding was that the non-parametric approach-PLSR with five components on eight spectral bands was the most robust method for CCC prediction. PLSR was reported superior to VIs (Inoue et al., 2016), and other non-parametric regression methods (Atzberger et al., 2010) to assess the CCC of crops and natural grasslands. However, it is worth noting that the input data used to calibrate the models bound the performance of non-parametric approaches (Delegido et al., 2011).

This study did not find a significant difference in accuracy between the physical-based method-INFORM inversion using LUT ($R^2 = 0.67$) and the SNAP toolbox approach ($R^2 = 0.66$), although INFORM was less biased (-0.101) than SNAP toolbox approach (-0.1632). These findings suggest that inversion of RTMs either using LUT or by applying statistical methods have comparable predictive accuracy in retrieving CCC from remote sensing data. The advantage of these approaches over other methods is that they minimize the over and/or underestimation of low and high CCC values. The predictions made by INFORM and SNAP toolbox follows the 1:1 relationship (Fig. 4) and may be preferred methods for precise estimation of CCC over large areas. However, physical-based models inversion demands vegetation structural characteristics information for the simulation of synthetic spectra, which requires extra effort to acquire.

This suggests that the statistical approaches, which are found sufficiently robust, accurate, and simple in this study, maybe the alternative approaches to run continuously in near-real-time across biomes (Delegido et al., 2011). However, caution must be applied, as the findings of statistical approaches are affected by the size and type of training datasets used. The calibration should be made based on *in situ* data collected across a broad range of vegetation types to obtain an accurate and precise prediction of CCC at a regional and global scale.

The maps generated by the four selected methods illustrate well the spatial variation of CCC across the test site. No visual differences were observed in the pattern of CCC distribution in the four CCC maps (Fig. 5), which confirms that canopy chlorophyll content can be estimated using Sentinel-2 imagery. However, when we investigated the

differences through image subtraction, the product from the SNAP toolbox was found to be deviating from the other products (Fig. 8).

However, the CCC record by PLSR is as low as 0.012 g/m2 and by SNAP toolbox reached as high as 4.35 g/m^2, and showed relatively higher frequency for those extreme values compared to the other two methods (Fig. 7). It seems possible that these results are due to the systematic over and underestimation nature of the two methods. The method in the SNAP toolbox is based on the PROSAIL model simulation, which assumes a homogeneous canopy structure (Huemmrich, 2001) that will be confounded by the heterogeneous forest canopy found in (semi-)natural forest. The minimum CCC value observed in PLSR generated map casts a shadow over the transferability of the method, which is based on a limited *in situ* dataset, to a larger spatial scale. The CCC range (0.22–4.35 g/m^2) obtained by the SNAP toolbox (4.35 g/m^2) was much higher than a similar study in temperate broadleaved forests founding CCC ranging from 0.04 to 2.63 g/m2 using PROSAIL (Singh and Sarnam, 2018). This might be partly attributed to the difference in phenological conditions of the vegetation studied besides the systematic over and underestimation nature of the algorithm.

5. Conclusion

There is a multitude of statistical and physical-based methods for the prediction of CCC from remote sensing data in the literature. However, previous studies primarily focus on the development of new techniques and lack a comprehensive comparison of methods to predict CCC from recently launched high-resolution imageries. This study tested the feasibility of a broad spectrum of methods from both statistical and physical-based approaches for mapping CCC of a heterogeneous mixed mountain forest from Sentinel-2 data. In general, methods which utilize remote sensing data from the red and red-edge region are superior in predicting CCC. Among the tested vegetation indices, mSR3 using central wavelength at 865 &665, mSR2 of 865 & 704 wavelength and $CI_{red\text{-}edge}$ based on 783 & 704 central wavelengths, PLSR on eight bands of Sentinel-2 with five components generate the most accurate CCC prediction than all the other statistical methods. Radiative transfer models inversion using LUT and by applying ANN (SNAP toolbox) provided similar accuracy, though INFORM inversion is less biased than SNAP toolbox.

Taken together, these results suggest that the CCC maps derived from Sentinel-2 imagery will enable a spatial assessment of terrestrial ecosystems condition by mapping CCC. The findings will be of interest to investigate the effectiveness of the proposed methods to quantify CCC of different vegetation types to explore the use of Sentinel-2 data to provide practical means for long-term terrestrial ecosystem monitoring efforts across the globe. To determine the operationally feasible method (s) that can be applied for retrieval of CCC in different ecosystems, further evaluation of the methods will be performed and reported in the near feature.

CRediT authorship contribution statement

Abebe Mohammed Ali: Conceptualization, Methodology, Formal analysis, Software, Writing - original draft, Visualization, Investigation, Validation. **Roshanak Darvishzadeh:** Methodology, Software, Writing - review & editing. **Andrew Skidmore:** Methodology, Supervision, Writing - review & editing. **Tawanda W. Gara:** Data curation. **Brian O'Connor:** Writing - review & editing. **Claudia Roeoesli:** Writing - review & editing. **Marco Heurich:** Supervision. **Marc Paganini:** Methodology, Supervision.

Declaration of Competing Interest

None.

Appendix A

Vegetation indices and CCC correlation
See Fig. A1.

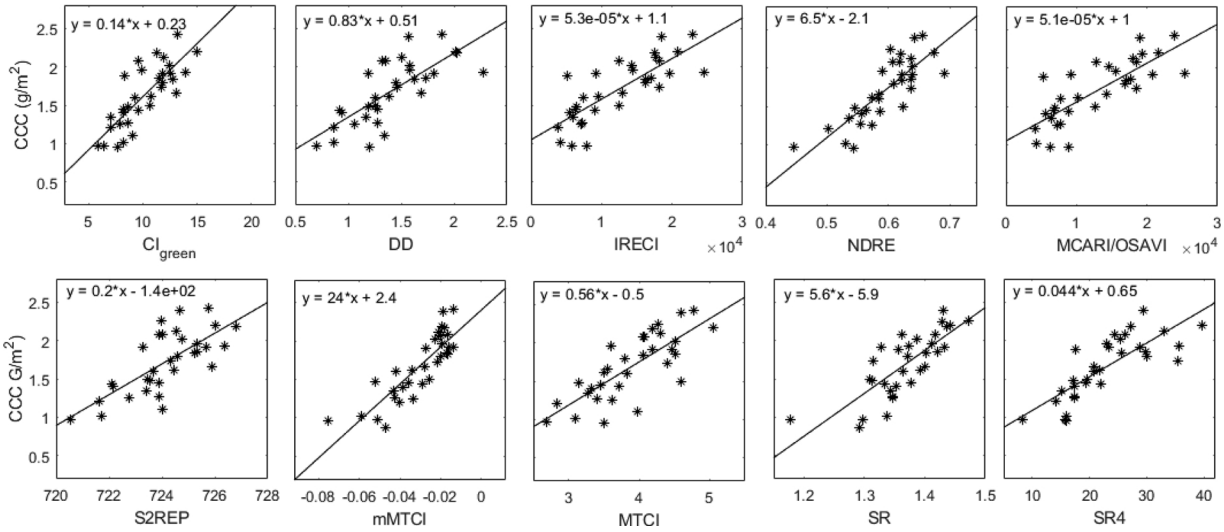

Fig. A1. Relationship between measured canopy chlorophyll content (CCC) (n = 32) and vegetation indices (VIs).

Appendix B

Measured *vs* predicted CCC scatter plots
See Fig. B1.

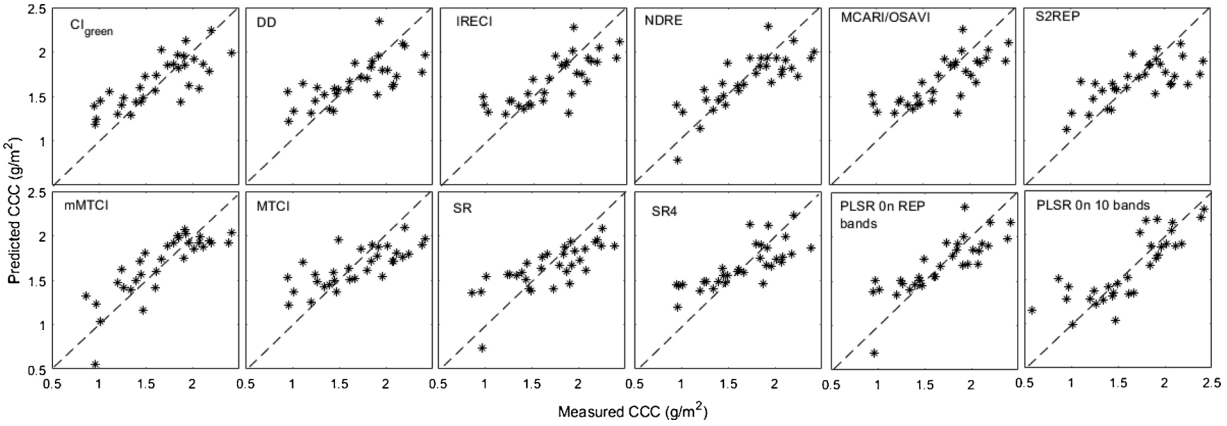

Fig. B1. Scatter plots of the *in situ* CCC and predictions made by different methods. Broken lines show the 1:1 relationship between the field measured and predicted values of CCC.

References

Ali, A.M., Darvishzadeh, R., Skidmore, A.K., van Duren, I., Heiden, U., Heurich, M., 2016a. Estimating leaf functional traits by inversion of PROSPECT: assessing leaf dry matter content and specific leaf area in mixed mountainous forest. Int. J. Appl. Earth Obs. Geoinf. 45, 66–76.

Ali, A.M., Skidmore, A.K., Darvishzadeh, R., van Duren, I., Holzwarth, S., Mueller, J., 2016b. Retrieval of forest leaf functional traits from HySpex imagery using radiative transfer models and continuous wavelet analysis. ISPRS J. Photogramm. Remote. Sens. 122, 68–80.

Asner, G.P., 1998. Biophysical and biochemical sources of variability in canopy reflectance (vol 64, pg 234, 1997). Remote Sens. Environ. 65, 225–226.

Asner, G.P., Martin, R.E., Carranza-Jiménez, L., Sinca, F., Tupayachi, R., Anderson, C.B., Martinez, P., 2014. Functional and biological diversity of foliar spectra in tree canopies throughout the Andes to Amazon region. New Phytol. 204, 127–139.

Atzberger, C., 2001. Development of an Invertible Forest Reflectance Model: The INFOR-Model. Decade of Trans-European Remote Sensing Cooperation, pp. 39–44.

Atzberger, C., Guérif, M., Baret, F., Werner, W., 2010. Comparative analysis of three chemometric techniques for the spectroradiometric assessment of canopy chlorophyll content in winter wheat. Comput. Electron. Agric. 73, 165–173.

Atzberger, C., Darvishzadeh, R., Schlerf, M., Le Maire, G., 2013. Suitability and adaptation of PROSAIL radiative transfer model for hyperspectral grassland studies. Remote. Sens. Lett. 4, 56–65.

Atzberger, C., Darvishzadeh, R., Immitzer, M., Schlerf, M., Skidmore, A., le Maire, G., 2015. Comparative analysis of different retrieval methods for mapping grassland leaf area index using airborne imaging spectroscopy. Int. J. Appl. Earth Obs. Geoinf. 43, 19–31.

Baret, F., Guyot, G., Major, D.J., 1989. TSAVI: a vegetation index which minimizes soil brightness effects on LAI and APAR estimation. 12th Canadian Symposium on Remote Sensing Geoscience and Remote Sensing Symposium, 10–14 July 1989 1355–1358.

Baret, F., Buis, S., 2008. Estimating canopy characteristics from remote sensing observations: review of methods and associated problems. Advances in Land Remote Sensing: System, Modeling, Inversion and Application. pp. 173–201.

Baret, F., 2016. S2ToolBox Level 2 Products: LAI, FAPAR, FCOVER: ATBD Used to Compute LAI, FAPAR and FVC, from SENTINEL2 Top of Canopy Reflectance Data That is Implemented in the SENTINEL2 Toolbox.

Barnes, E.M., Clarke, T.R., Richards, S.E., Colaizzi, P.D., Haberl, J., Kostrzewski, M., et al., 2000. Coincident detection of crop water stress, nitrogen status and canopy density using ground based Muhttps. the Fifth International Conference on Precision Agriculture.

Broge, N.H., Leblanc, E., 2001. Comparing prediction power and stability of broadband and hyperspectral vegetation indices for estimation of green leaf area index and canopy chlorophyll density. Remote Sens. Environ. 76, 156–172.

Chemura, A., Mutanga, O., Odindi, J., 2017. Empirical modeling of leaf chlorophyll content in coffee (Coffea Arabica) plantations with sentinel-2 MSI data: effects of spectral settings, spatial resolution, and crop canopy cover. IEEE J. Selected Top. Appl. Earth Observ. Remote Sens. 10, 5541–5550.

Clevers, J.G.P.W., Gitelson, A.A., 2012. Using the Red-Edge Bands on Sentinel-2 for Retrieving Canopy Chlorophyll and Nitrogen Content. European Space Agency, (Special Publication) ESA SP.

Clevers, J.G.P.W., Kooistra, L., van den Brande, M.M.M., 2017. Using Sentinel-2 Data for Retrieving LAI and Leaf and Canopy Chlorophyll Content of a Potato Crop. Remote Sensing, pp. 9.

Combal, B., Baret, F., Weiss, M., Trubuil, A., Mace, D., Pragnere, A., et al., 2003. Retrieval of canopy biophysical variables from bidirectional reflectance – using prior information to solve the ill-posed inverse problem. Remote Sens. Environ. 84, 1–15.

Croft, H., Chen, J.M., Zhang, Y., Simic, A., 2013. Modelling leaf chlorophyll content in broadleaf and needle leaf canopies from ground, CASI, Landsat TM 5 and MERIS reflectance data. Remote Sens. Environ. 133, 128–140.

Cui, S., Zhou, K., 2017. A comparison of the predictive potential of various vegetation indices for leaf chlorophyll content. Earth Sci. Inform. 10, 169–181.

Curran, P.J., 1989. Remote-sensing of foliar chemistry. Remote Sens. Environ. 30, 271–278.

Curran, P.J., Dungan, J.L., Gholz, H.L., 1990. Exploring the relationship between reflectance red edge and chlorophyll content in slash pine. Tree Physiol. 7, 33–48.

Darvishzadeh, R., Skidmore, A., Atzberger, C., van Wieren, S., 2008a. Estimation of vegetation LAI from hyperspectral reflectance data: effects of soil type and plant architecture. Int. J. Appl. Earth Obs. Geoinf. 10, 358–373.

Darvishzadeh, R., Skidmore, A., Schlerf, M., Atzberger, C., 2008b. Inversion of a radiative transfer model for estimating vegetation LAI and chlorophyll in a heterogeneous grassland. Remote Sens. Environ. 112, 2592–2604.

Darvishzadeh, R., Skidmore, A., Schlerf, M., Atzberger, C., Corsi, F., Cho, M., 2008c. LAI and chlorophyll estimation for a heterogeneous grassland using hyperspectral measurements. ISPRS J. Photogramm. Remote. Sens. 63, 409–426.

Darvishzadeh, R., Skidmore, A., Abdullah, H., Cherenet, E., Ali, A., Wang, T., et al., 2019a. Mapping leaf chlorophyll content from Sentinel-2 and RapidEye data in spruce stands using the invertible forest reflectance model. Int. J. Appl. Earth Obs. Geoinf. 79, 58–70.

Darvishzadeh, R., Wang, T., Skidmore, A., Vrieling, A., O'Connor, B., Gara, T.W., et al., 2019b. Analysis of sentinel-2 and rapid eye for retrieval of leaf area index in a saltmarsh using a radiative transfer model. Remote Sens. 11, 671.

Dash, J., Curran, P.J., 2004. The MERIS terrestrial chlorophyll index. Int. J. Remote Sens. 25, 5403–5413.

Datt, B., 1999. A new reflectance index for remote sensing of chlorophyll content in higher plants: tests using Eucalyptus leaves. J. Plant Physiol. 154, 30–36.

Daughtry, C.S.T., Walthall, C.L., Kim, M.S., de Colstoun, E.B., McMurtrey, J.E., 2000. Estimating corn leaf chlorophyll concentration from leaf and canopy reflectance. Remote Sens. Environ. 74, 229–239.

Dawson, T.P., Curran, P.J., 1998. Technical note A new technique for interpolating the reflectance red edge position. Int. J. Remote Sens. 19, 2133–2139.

Dawson, T.P., Curran, P.J., Plummer, S.E., 1998. LIBERTY - modeling the effects of leaf biochemical concentration on reflectance spectra. Remote Sens. Environ. 65, 50–60.

Delegido, J., Verrelst, J., Alonso, L., Moreno, J., 2011. Evaluation of Sentinel-2 red-edge bands for empirical estimation of green LAI and chlorophyll content. Sensors 11, 7063–7081.

Dian, Y., Le, Y., Fang, S., Xu, Y., Yao, C., Liu, G., 2016. Influence of spectral bandwidth and position on chlorophyll content retrieval at leaf and canopy levels. J. Indian Soc. Remote. Sens. 44, 583–593.

Féret, J.B., François, C., Gitelson, A., Asner, G.P., Barry, K.M., Panigada, C., et al., 2011. Optimizing spectral indices and chemometric analysis of leaf chemical properties using radiative transfer modeling. Remote Sens. Environ. 115, 2742–2750.

Féret, J.B., Gitelson, A.A., Noble, S.D., Jacquemoud, S., 2017. PROSPECT-D: towards modeling leaf optical properties through a complete lifecycle. Remote Sens. Environ. 193, 204–215.

Frampton, W.J., Dash, J., Watmough, G., Milton, E.J., 2013. Evaluating the capabilities of Sentinel-2 for quantitative estimation of biophysical variables in vegetation. ISPRS J.

Photogramm. Remote. Sens. 82, 83–92.
Gitelson, A.A., Merzlyak, M.N., 1997. Remote estimation of chlorophyll content in higher plant leaves. Int. J. Remote Sens. 18, 2691–2697.
Gitelson, A.A., Viña, A., Ciganda, V., Rundquist, D.C., Arkebauer, T.J., 2005. Remote estimation of canopy chlorophyll content in crops. Geophys. Res. Lett. 32 n/a-n/a.
Gitelson, A.A., Peng, Y., Arkebauer, T.J., Suyker, A.E., 2015. Productivity, absorbed photosynthetically active radiation, and light use efficiency in crops: implications for remote sensing of crop primary production. J. Plant Physiol. 177, 100–109.
Haboudane, D., Miller, J.R., Tremblay, N., Zarco-Tejada, P.J., Dextraze, L., 2002. Integrated narrow-band vegetation indices for prediction of crop chlorophyll content for application to precision agriculture. Remote Sens. Environ. 81, 416–426.
Haboudane, D., Miller, J.R., Pattey, E., Zarco-Tejada, P.J., Strachan, I.B., 2004. Hyperspectral vegetation indices and novel algorithms for predicting green LAI of crop canopies: modeling and validation in the context of precision agriculture. Remote Sens. Environ. 90, 337–352.
Heurich, M., Beudert, B., Rall, H., Křenová, Z., 2010. Nationalnational parks as model regions for interdisciplinary long-term ecological research: the Bavarian Forest and Šumavá national parks underway to transboundary ecosystem research. In: MÜLLER, F., BAESSLER, C., SCHUBERT, H., KLOTZ, S. (Eds.), Long-Term Ecological Research: Between Theory and Application. Springer Netherlands, Dordrecht.
Homolova, L., Malenovský, Z., Clevers, J.G., García-Santos, G., Schaepman, M.E., 2013. Review of optical-based remote sensing for plant trait mapping. Ecol. Complex. 15, 1–16.
Houborg, R., Cescatti, A., Migliavacca, M., Kustas, W.P., 2013. Satellite retrievals of leaf chlorophyll and photosynthetic capacity for improved modeling of GPP. Agric. For. Meteorol. 117, 10–23.
Houborg, R., McCabe, M., Cescatti, A., Gao, F., Schull, M., Gitelson, A., 2015. Joint leaf chlorophyll content and leaf area index retrieval from Landsat data using a regularized model inversion system (REGFLEC). Remote Sens. Environ. 159, 203–221.
Huemmrich, K.F., 2001. The GeoSail model: a simple addition to the SAIL model to describe discontinuous canopy reflectance. Remote Sens. Environ. 75, 423–431.
Huete, A.R., 1988. A soil-adjusted vegetation index (Savi). Remote Sens. Environ. 25, 295–309.
Hunt, E.R., Doraiswamy, P.C., McMurtrey, J.E., Daughtry, C.S., Perry, E.M., Akhmedov, B., 2012. A visible band index for remote sensing leaf chlorophyll content at the Canopy scale. Int. J. Appl. Earth Obs. Geoinf. 21, 103–112.
Inoue, Y., Sakaiya, E., Zhu, Y., Takahashi, W., 2012. Diagnostic mapping of canopy nitrogen content in rice based on hyperspectral measurements. Remote Sens. Environ. 126, 210–221.
Inoue, Y., Guérif, M., Baret, F., Skidmore, A., Gitelson, A., Schlerf, M., et al., 2016. Simple and robust methods for remote sensing of canopy chlorophyll content: a comparative analysis of hyperspectral data for different types of vegetation. Plant Cell Environ. 39, 2609–2623.
Jacquemoud, S., Baret, F., 1990. Prospect – a model of leaf optical-properties spectra. Remote Sens. Environ. 34, 75–91.
Jacquemoud, S., Verhoef, W., Baret, F., Bacour, C., Zarco-Tejada, P.J., Asner, G.P., et al., 2009. PROSPECT plus SAIL models: a review of use for vegetation characterization. Remote Sens. Environ. 113, S56–S66.
Ju, C.H., Tian, Y.C., Yao, X., Cao, W.X., Zhu, Y., Hannaway, D., 2010. Estimating leaf chlorophyll content using red edge parameters. Pedosphere 20, 633–644.
Korus, A., 2013. Effect of preliminary and technological treatments on the content of chlorophylls and carotenoids in kale (Brassica oleracea L. Var. Acephala). J. Food Process. Preserv. 37, 335–344.
Lehnert, L.W., Bassler, C., Brandl, R., Burton, P.J., Muller, J., 2013. Conservation value of forests attacked by bark beetles: highest number of indicator species is found in early successional stages. J. Nat. Conserv. 21, 97–104.
Li, L., Ren, T., Ma, Y., Wei, Q., Wang, S., Li, X., et al., 2016. Evaluating chlorophyll density in winter oilseed rape (Brassica napus L.) using canopy hyperspectral red-edge parameters. Comput. Electron. Agric. 126, 21–31.
Li, X., Liu, X., Liu, M., Wang, C., Xia, X., 2015. A hyperspectral index sensitive to subtle changes in the canopy chlorophyll content under arsenic stress. Int. J. Appl. Earth Obs. Geoinf. 36, 41–53.
Li, Z., Xu, D., Guo, X., 2014. Remote sensing of ecosystem health: opportunities, challenges, and future perspectives. Sensors (Basel, Switzerland) 14, 21117–21139.
Liang, L., Qin, Z., Zhao, S., Di, L., Zhang, C., Deng, M., et al., 2016. Estimating crop chlorophyll content with hyperspectral vegetation indices and the hybrid inversion method. Int. J. Remote Sens. 37, 2923–2949.
Liang, S., 2007. Recent developments in estimating land surface biogeophysical variables from optical remote sensing. Prog. Phys. Geogr. 31, 501–516.
Luo, X., Croft, H., Chen, J.M., Bartlett, P., Staebler, R., Froelich, N., 2018. Incorporating leaf chlorophyll content into a two-leaf terrestrial biosphere model for estimating carbon and water fluxes at a forest site. Agric. For. Meteorol. 248, 156–168.
Ma, M., Shi, R., Liu, P., Wang, H., Gao, W., 2014. The impacts of bandwidths on the estimation of leaf chlorophyll concentration using normalized difference vegetation indices. Proceedings of SPIE - The International Society for Optical Engineering.
Malenovský, Z., Martin, E., Homolová, L., Gastellu-Etchegorry, J.-P., Zurita-Milla, R., Schaepman, M.E., et al., 2008. Influence of woody elements of a Norway spruce canopy on nadir reflectance simulated by the DART model at very high spatial resolution. Remote Sens. Environ. 112, 1–18.
Niemann, K.O., Quinn, G., Goodenough, D.G., Visintini, F., Loos, R., 2012. Addressing the effects of canopy structure on the remote sensing of foliar chemistry of a 3-dimensional, radiometrically porous surface. IEEE J. Sel. Top. Appl. Earth Obs. Remote. Sens. 5, 584–593.
Okuda, K., Taniguchi, K., Miura, M., Obata, K., Yoshioka, H., 2016. Application of vegetation isoline equations for simultaneous retrieval of leaf area index and leaf chlorophyll content using reflectance of red edge band. Proceedings of SPIE - The International Society for Optical Engineering.
Ollinger, S.V., 2011. Sources of variability in canopy reflectance and the convergent properties of plants. New Phytol. 189, 375–394.
Peng, Y., Gitelson, A.A., 2011. Application of chlorophyll-related vegetation indices for remote estimation of maize productivity. Agric. For. Meteorol. 151, 1267–1276.
Rocha, A.D., Groen, T.A., Skidmore, A.K., Darvishzadeh, R., Willemen, L., 2017. The Naïve Overfitting Index Selection (NOIS): a new method to optimize model complexity for hyperspectral data. ISPRS J. Photogramm. Remote. Sens. 133, 61–74.
Rosema, A., Verhoef, W., Noorbergen, H., Borgesius, J.J., 1992. A new forest light interaction-model in support of forest monitoring. Remote Sens. Environ. 42, 23–41.
Sæbø, S., Almøy, T., Flatberg, A., Aastveit, A.H., Martens, H., 2008. LPLS-regression: a method for prediction and classification under the influence of background information on predictor variables. Chemom. Intell. Lab. Syst. 91, 121–132.
Scales, J.A., Tenorio, L., 2001. Prior information and uncertainty in inverse problems. Geophysics 66, 389–397.
Schlerf, M., Atzberger, C., 2006. Inversion of a forest reflectance model to estimate structural canopy variables from hyperspectral remote sensing data. Remote Sens. Environ. 100, 281–294.
Silveyra Gonzalez, R., Latifi, H., Weinacker, H., Dees, M., Koch, B., Heurich, M., 2018. Integrating LiDAR and high-resolution imagery for object-based mapping of forest habitats in a heterogeneous temperate forest landscape. Int. J. Remote Sens. 39, 8859–8884.
Singh, D.S., Sarnam, 2018. Geospatial modeling of canopy chlorophyll content using high spectral resolution satellite data in himalayan forests. Clim. Chang. Environ. Sustain. 6.
Skidmore, A.K., 2002. Taxonomy of environmental models in the spatial sciences. In: SKIDMORE, A. (Ed.), Environmental Modelling with GIS and Remote Sensing. Taylor & Francis.
Sun, Q., Jiao, Q.J., Dai, H.Y., 2018. Evaluating the capabilities of vegetation spectral indices on chlorophyll content estimation at Sentinel-2 spectral resolutions. Mippr 2017: Remote Sensing Image Processing, Geographic Information Systems, and Other Applications. pp. 10611.
Tong, A., He, Y., 2017. Estimating and mapping chlorophyll content for a heterogeneous grassland: comparing prediction power of a suite of vegetation indices across scales between years. ISPRS J. Photogramm. Remote. Sens. 126, 146–167.
Verhoef, W., 1984. Light-scattering by leaf layers with application to canopy reflectance modeling - the sail model. Remote Sens. Environ. 16, 125–141.
Verrelst, J., Schaepman, M.E., Malenovský, Z., Clevers, J.G.P.W., 2010. Effects of woody elements on simulated canopy reflectance: implications for forest chlorophyll content retrieval. Remote Sens. Environ. 114, 647–656.
Verrelst, J., Muñoz, J., Alonso, L., Delegido, J., Rivera, J.P., Camps-Valls, G., Moreno, J., 2012. Machine learning regression algorithms for biophysical parameter retrieval: opportunities for Sentinel-2 and -3. Remote Sens. Environ. 118, 127–139.
Verrelst, J., Camps-Valls, G., Muñoz-Marí, J., Rivera, J.P., Veroustraete, F., Clevers, J.G.P.W., Moreno, J., 2015. Optical remote sensing and the retrieval of terrestrial vegetation bio-geophysical properties – a review. ISPRS J. Photogramm. Remote. Sens. 108, 273–290.
Vincini, M., Amaducci, S., Frazzi, E., 2014. Empirical estimation of leaf chlorophyll density in winter wheat canopies using Sentinel-2 spectral resolution. IEEE Trans. Geosci. Remote. Sens. 52, 3220–3235.
Vincini, M., Calegari, F., Casa, R., 2016. Sensitivity of leaf chlorophyll empirical estimators obtained at Sentinel-2 spectral resolution for different canopy structures. Precis. Agric. 17, 313–331.
Wang, Z., Skidmore, A.K., Wang, T., Darvishzadeh, R., Heiden, U., Heurich, M., et al., 2017. Canopy foliar nitrogen retrieved from airborne hyperspectral imagery by correcting for canopy structure effects. Int. J. Appl. Earth Obs. Geoinf. 54, 84–94.
Widlowski, J.-L., Mio, C., Disney, M., Adams, J., Andredakis, I., Atzberger, C., et al., 2015. The fourth phase of the radiative transfer model intercomparison (RAMI) exercise: Actual canopy scenarios and conformity testing. Remote Sens. Environ. 169, 418–437.
Wu, C., Niu, Z., Gao, S., 2012. The potential of the satellite derived green chlorophyll index for estimating midday light use efficiency in maize, coniferous forest and grassland. Ecol. Indic. 14, 66–73.
Wu, C.Y., Niu, Z., Tang, Q., Huang, W.J., 2008. Estimating chlorophyll content from hyperspectral vegetation indices: modeling and validation. Agric. For. Meteorol. 148, 1230–1241.
Yanez-Rausell, L., Malenovsky, Z., Rautiainen, M., Clevers, J.G.P.W., Lukes, P., Hanus, J., Schaepman, M.E., 2015. Estimation of spruce needle-leaf chlorophyll content based on DART and PARAS canopy reflectance models. IEEE J. Sel. Top. Appl. Earth Obs. Remote. Sens.
Zhang, T., 2001. A leave-one-out cross validation bound for kernel methods with applications in learning. Computational Learning Theory, Proceedings 2111, 427–443.
Zhao, C., Wang, Z., Wang, J., Huang, W., Guo, T., 2011. Early detection of canopy nitrogen deficiency in winter wheat (Triticum aestivum L.) based on hyperspectral measurement of canopy chlorophyll status. N. Z. J. Crop Hortic. Sci. 39, 251–262.
Zou, X., Hernández-Clemente, R., Tammeorg, P., Lizarazo Torres, C., Stoddard, F.L., Mäkelä, P., et al., 2015. Retrieval of leaf chlorophyll content in field crops using narrow-band indices: effects of leaf area index and leaf mean tilt angle. Int. J. Remote Sens. 36, 6031–6055.